

Levels in  $^{99}\text{Zr}$  observed in the decay of  $^{99}\text{Y}$ 

G. Lhersonneau

*INFN, Laboratori Nazionali di Legnaro, Viale dell'Università 2, I-35020 Legnaro (PD), Italy*

S. Brant

*Department of Physics, Faculty of Science, University of Zagreb, Bijenicka 32, 10000 Zagreb, Croatia*

(Received 28 May 2004; published 28 September 2005)

A new investigation of the decay scheme of  $^{99}\text{Y}$  to  $^{99}\text{Zr}$  removes minor discrepancies between decay and prompt-fission data. The existence of a strongly coupled band on the 725-keV level postulated in an earlier  $\beta$ -decay work is not confirmed. Calculations in the interacting boson fermion framework allow an alternative interpretation of the even-parity levels above 500 keV. Still, the nature of most of these levels above remains unclear.

DOI: [10.1103/PhysRevC.72.034308](https://doi.org/10.1103/PhysRevC.72.034308)

PACS number(s): 23.20.Lv, 21.60.Fw, 27.60.+j

## I. INTRODUCTION

The neutron-rich nucleus  $^{99}\text{Zr}$  is located at a transition between the region of strong subshell closures centered on  $^{96}\text{Zr}$  and the deformation region with  $\beta = 0.3\text{--}0.4$  starting with  $^{100}\text{Zr}$ . The dramatic lowering of the  $2_1^+$  energies from 1223 keV in  $^{98}\text{Zr}_{58}$  to 212 keV in  $^{100}\text{Zr}_{60}$  has been understood as the result of relative shifts of spherical and deformed minima of the potential energy surfaces [1]. The lowest lying levels of the intermediate  $N = 59$  isotones were proposed to be spherical, first based on level structure arguments. They have been studied in the framework of the interacting boson fermion and interacting boson fermion-fermion models (IBFM) [2–5]. A direct evidence for the spherical shape of the  $^{99}\text{Zr}$  ground state (g.s.) has been obtained recently by collinear laser spectroscopy of Zr isotopes [6]. In addition,  $3/2^-$  (614 keV) and  $3/2^+$  (725 keV) deformed band heads were also proposed in  $^{99}\text{Zr}$  [1]. Nevertheless, the states observable in  $\beta$  decay span a limited spin range. It had to be awaited for prompt-fission studies performed with large Ge-arrays such as GAMMASPHERE [7] or EUROBALL [8,9] to observe more developed band structures and to firmly identify the  $[404]9/2$  neutron Nilsson orbital. After these new experiments it becomes of interest to improve the  $\beta$ -decay data, especially to remove a few inconsistencies between branching ratios reported in Refs. [1] and [8]. Moreover,  $\beta$  decay remains the only method to access low-spin levels far from the yrast line that are too weakly populated in prompt fission.

The last published full decay scheme of  $^{99}\text{Y}$  to  $^{99}\text{Zr}$  has been constructed from  $\gamma$ -ray singles and  $\gamma$ - $\gamma$  coincidences recorded after online mass separation of fission products at the OSTIS and ISOLDE online mass-separators [1]. New  $\gamma$ - $\gamma$  coincidence data from the decays of  $A = 99$  isobars were later obtained at the IGISOL facility in Jyväskylä, Finland, but only the new levels in relationship with the odd-parity band in  $^{99}\text{Zr}$  have been reported so far [10]. An updated and comprehensive decay scheme is presented here.

## II. EXPERIMENT

As experimental details can be found in previous publications [10,11] only a brief summary is given here. The

levels of  $^{99}\text{Zr}$  are populated in the  $\beta$  decay of online mass separated  $^{99}\text{Y}$ , a well deformed nucleus with  $I^\pi = 5/2^+$  [12]. The specific features of the ion-guide technique used for the experiments are a release time of the order of the  $ms$  and the absence of constraints bound to the chemical properties of the elements to be separated. To a good approximation the beam intensities of mass-separated isobars are proportional to the production cross sections in the fission reaction used, here 25 MeV protons on natural uranium. Following a simple parametrization [13] the production cross sections for  $A = 99$  isobars in this reaction have a FWHM of  $\Delta Z = 1.65$  and peak at  $Z = 40.2$ . Contaminations by  $^{99}\text{Rb}$  and  $^{99}\text{Sr}$  activities are thus much lower than during the measurements of Ref. [1], where  $^{99}\text{Y}$  was formed only during collection of the  $A = 99$  isobars as a  $\beta$ -decay product of the mass separated  $^{99}\text{Rb}$  and  $^{99}\text{Sr}$  nuclei.

The detection setup was an array of nine Compton-suppressed Ge detectors supplemented with a low-energy planar Ge detector. A symmetric  $\gamma$ - $\gamma$  matrix with the nine Ge detectors was used for lines above about 80 keV. The partial projections gated by the 614- and 725-keV transitions (Figs. 1 and 2) demonstrate the improvement of spectrum quality with respect to Ref. [1]. The relative efficiency for coincidence pairs was determined independently of standards by using conservation of  $\gamma$ -ray flow in the cascades present in selected gates. The coincidence time window allowed 77% of the coincidences across the 252-keV level ( $t_{1/2} = 293$  ns) to be recorded. As a rule, the relative intensities of transitions have been extracted from the number of coincidences. The intensity of the 130-keV line measured in Ref. [1] has been used for normalization. The intensities of the ground-state transitions of 576, 658, and 885 keV were also obtained from coincidences as the relatively strong  $\gamma$ -ray population of these levels allows to determine their branching ratios. For other g.s. transitions the intensities obtained from the singles spectra of Ref. [1] have been adopted. Another energy-energy matrix with the low-energy planar detector against the nine other Ge detectors was used for the low-energy range, allowing the observation of the  $\gamma$  rays in coincidence with  $K_\alpha$  rays of the various isobars. Electron conversion has been taken into account for the strongest transitions below 200 keV. When

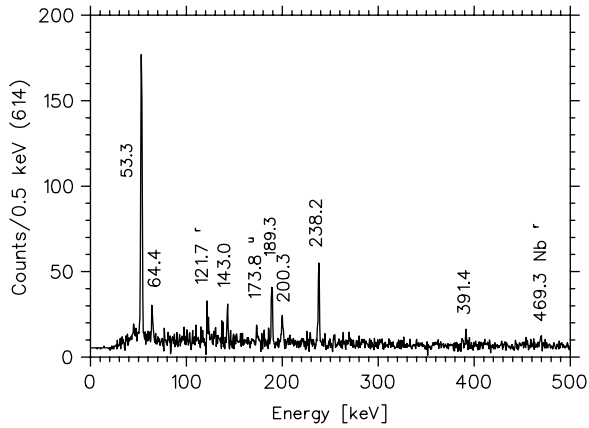


FIG. 1. Projection gated by the 614-keV transition obtained with the nine-detector array. A constant visible at the very left has been added to avoid display of negative counts. The labels r and u refer to random coincidences and an unassigned transition, respectively. Other lines are placed in the scheme.

not experimentally available, theoretical coefficients for the multipolarity of lowest order possible have been used.

### III. RESULTS

The transitions assigned to the decay of  $^{99}\text{Y}$  are listed in Table I and the level scheme is shown in Figs. 3(a)–3(c). Transition energies and intensities are usually in good agreement with those reported in the previous decay study. All transitions with more than 1% relative intensity units in the decay of  $^{99}\text{Y}$ , except for a single one, are confirmed. The coincidences reported in Ref. [1] for the transitions at 206.5 and 207.4 keV in fact could indicate a single transition from the level at 1006 keV to the level at 851 keV. However, none of them has been found in the present work. As a consequence of lack of other confirmed transitions the levels at 755 keV (see

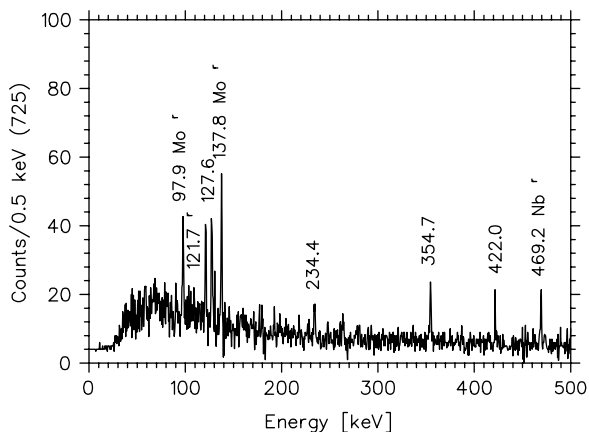


FIG. 2. Projection gated by the 725-keV transition obtained with the nine detector array. See caption of Fig. 1. The sharp line at the foot of the 127.6 keV peak is a residual of the random coincidence with the 130.2-keV transition (not marked).

Ref. [10]) and 1024 keV are removed. The level at 1064.5 keV is replaced with a low-spin level at 1064.7 and another level at 1065.9 keV. The latter is identified by its decay branchings with the  $9/2^+$  level reported by Urban *et al.* [8].

We note a slight increase of the relative populations of the 576-, 851-, 852-, and 1588-keV levels with respect to Ref. [1]. This effect could indicate a new decay mode. It is indeed possible because  $^{99}\text{Y}$  is not only formed by radioactive fission but also delivered as a mass-separated beam. In this case it is tempting to invoke an as-yet-identified isomer in  $^{99}\text{Y}$ . Such an isomer could occur, for instance, in a spherical potential well. Although no definite evidence for spherical levels in  $^{99}\text{Y}$  has been reported so far, a low-lying spherical minimum of potential energy is expected by analogy with its even-even neighbors  $^{98}\text{Sr}$  and  $^{100}\text{Zr}$  [ $E(0_2^+) = 216$  and 331 keV, respectively] [14].

Beta feedings and  $\log(ft)$  values of the levels populated in the  $\beta$  decay of  $^{99}\text{Y}$  ( $I^\pi = 5/2^+$ ) are shown in Table II. There are only minor changes of no consequence on the deduced spins and parities. Thus, no definite new spin and parity assignments can be made on basis of  $\log(ft)$  values and  $\gamma$ -branching ratios. Calculated  $\beta$  feedings are sensitive to the amount of  $\gamma$  feeding that has possibly been overlooked and therefore they represent higher limits. We have considered that a calculated  $\beta$ -branch intensity of the order of the percent is large enough to establish a definite feeding corresponding to an allowed or first-forbidden transition, implying  $I = (3/2, 5/2, \text{ and } 7/2)$ . Even parity is thus firm for the level at 725 keV [ $\log(ft) = 5.6$ ] and probable for the 852-, 1588-, 2401-, and 2449-keV levels that have  $\log(ft)$  values not exceeding 6.0. Despite higher  $\log(ft)$  values the 762- and 1079-keV levels can also be regarded as having even parity owing to the presence of transitions to both the  $1/2^+$  g.s. and to the  $7/2_1^+$  state. Among these  $\beta$ -fed levels some exhibit a dominant  $\gamma$  branch to the  $1/2^+$  g.s. that favors  $3/2$  over  $5/2$ . It is indeed expected that a  $5/2$  state has easier alternative decays by dipole transitions to the  $3/2_1^+$  and  $7/2_1^+$  states. Thus, the 782- and 1064-keV levels are probable  $3/2$  states. We note that the only source for a  $3/2^-$  level is the deformed [541]3/2 orbital identified at 614 keV [1,8,10] and, consequently, the 782- and 1064-keV levels should have even parity.

In Ref. [1] the 725- and 852-keV levels have been assumed to form the bottom of a  $K = 3/2$  band. The branchings of the 725-keV level are much like those of the  $3/2^+$  level at 576 keV [8], making  $I^\pi(725) = 3/2^+$  indeed a reasonable choice. The only other assignment consistent with the  $\log(ft)$  value and the transition to the  $1/2^+$  ground state is  $I^\pi = 5/2^+$ . According to our data the 852-keV level has  $I^\pi = 3/2^+$  or  $5/2^+$ . It has been tentatively proposed as  $7/2^+$  in Ref. [8] but this spin and parity are ruled out by the transition to the  $3/2^-$  level and the level lifetime of 44(11) ps [15]. The existence of transitions to the  $3/2_1^+$  and  $7/2_1^+$  states, whereas the transition to the  $1/2^+$  g.s. has not been detected, together with the observation in prompt fission, favor  $5/2^+$  over  $3/2^+$ . A calculation of  $\beta$ -feeding intensities in the quasiparticle random phase approximation predicted the largest branch to populate a deformed  $3/2^+$  level. This was the basis for the interpretation of the 725- and 852-keV levels as being the  $K = 3/2$  and  $K + 1 = 5/2$  levels of a

TABLE I. List of  $\gamma$  rays assigned to the decay scheme of  $^{99}\text{Zr}$ . To obtain the probability of transitions for 100 decays multiply the relative intensity units by 0.469. To keep the table compact only the coincident transitions placed below the current listed transition (thus these defining the placement) are indicated.

| Energy [KeV] | Intensity | Placement |                   | Coincidences  |
|--------------|-----------|-----------|-------------------|---|
|              |           | From      | To                |   |
| 11.1         | 0.14 (4)  | 679       | 668 <sup>ab</sup> |   |
| 20.7         | 0.09 (5)  | 679       | 658 <sup>c</sup>  |   |
| 46.1 (2)     | 0.09 (3)  | 868       | 822 <sup>d</sup>  | (64), (143), (427)                                    |
| 53.3 (1)     | 2.4 (4)   | 668       | 614               | (189), 200, (1629), 1733                              |
| 64.4 (1)     | 0.19 (4)  | 679       | 614 <sup>ae</sup> | (46), (143)   |
| 66.6 (1)     | 0.55 (10) | 725       | 658 <sup>f</sup>  | 122, 536  |
| 82.2 (2)     | 0.77 (24) | (658)     | 576 <sup>g</sup>  | (576)   |
| 90.4 (1)     | 1.17 (20) | 852       | 762 <sup>h</sup>  | 122, 186, 454, 510, 576, 640, (762)                   |
| 91.7 (2)     | 1.32 (35) | 668       | 576               | 122, 454, 576   |
| 121.7 (1)    | 100       | 122       | 0                 |   |
| 127.6 (2)    | 0.44 (6)  | 852       | 725               | 725   |
| 130.2 (1)    | 15.4 (17) | 252       | 122               | 122   |
| 143.0 (3)    | 0.29 (5)  | 822       | 679 <sup>ae</sup> | (64), (130), (416), (427), 614                        |
| 149.0 (2)    | 0.34 (4)  | 725       | 576               | 122, 454, 576   |
| 186.1 (2)    | 0.83 (8)  | 762       | 576               | 90, 122, 454, 576                                     |
| 189.3 (3)    | 0.54 (5)  | 868       | 679 <sup>ai</sup> | (53), (92), 122, 130, (406), (416), (427), (536), 614 |
| 192.7 (2)    | 4.08 (50) | 851       | 658               | 122, 130, 406, 536                                    |
| 194.1 (2)    | 5.66(58)  | 852       | 658               | 122, 130, 406, 536                                    |
| 200.3 (3)    | 0.28 (5)  | 868       | 668 <sup>ae</sup> | (53), (92), (416), 614                                |
| 215.5 (2)    | 0.21 (4)  | 1066      | 851 <sup>j</sup>  | 122, 193, (275), 536                                  |
| 234.4 (3)    | 0.18 (5)  | 959       | 725               | (725)   |
| 238.2 (2)    | 0.48 (6)  | 852       | 614               | 614   |
| 261.6 (3)    | 0.34 (7)  | 1147      | 885               | (310), 885  |
| 274.9 (3)    | 1.41 (17) | 851       | 576 <sup>k</sup>  | 122, 130, 454, 576                                    |
| 276.6 (2)    | 4.96(56)  | 852       | 576               | 122, 130, (324), 454, 536                             |
| 282.6 (2)    | 0.66 (9)  | 1065      | 782               | 782   |
| 296.9 (2)    | 0.74 (10) | 1079      | 782               | 782   |
| 301.0 (3)    | 0.17 (4)  | 959       | 658               | (122), (536)  |
| 309.6 (2)    | 0.61 (9)  | 885       | 576               | 122, 454, 576   |
| 317.4 (3)    | 0.30 (5)  | 1079      | 762 <sup>l</sup>  | (122)   |
| 323.8 (3)    | 0.86 (12) | 576       | 252               | 122, 130  |
| 347.8 (2)    | 0.74 (10) | 1006      | 658               | 122, (406), 536                                       |
| 354.7 (3)    | 0.44 (9)  | 1079      | 725               | 725   |
| 391.4 (4)    | 0.14 (4)  | 1006      | 614               | 614   |
| 392.5 (3)    | 1.20 (17) | 1154      | 762               | 122, 640  |
| 405.9 (2)    | 4.50 (60) | 658       | 252               | 122, 130  |
| 407.7 (3)    | 0.64 (10) | 1066      | 658               | 122, 130, 536   |
| 415.6 (2)    | 1.70 (20) | 668       | 252               | 122, 130  |
| 421.4 (3)    | 0.34 (5)  | 1079      | 658               | (122), 536  |
| 422.0 (4)    | 0.27 (8)  | 1147      | 725               | (724)   |
| 426.7 (3)    | 0.65 (11) | 679       | 252               | 122, 130  |
| 429.7 (3)    | 0.62 (8)  | 1006      | 576               | 122, 454, 576   |
| 448.1 (3)    | 0.20 (5)  | 1230      | 782               | (782)   |
| 454.0 (1)    | 12.0 (14) | 576       | 122               | 122   |
| 472.7 (2)    | 1.90 (30) | 725       | 252               | 122, 130  |
| 475.3 (4)    | 0.24 (10) | 1051      | 576               | (122), (454), (576)                                   |
| 476.2 (3)    | 0.15 (5)  | (1325)    | 658)              | (122), (193), (536)                                   |
| 509.6 (2)    | 0.73 (10) | 762       | 252               | 122, 130  |
| 536.2 (1)    | 23.8 (29) | 658       | 122               | 122   |
| 546.0 (3)    | 0.65 (11) | 668       | 122               | 122   |
| 570.6 (3)    | 0.97 (16) | 1147      | 576               | 122, 454, 576   |
| 572.3 (4)    | 0.63 (10) | 1230      | 658               | 122, (130), (406), 536                                |
| 575.7 (1)    | 21.0 (35) | 576       | 0                 |   |
| 600.1 (2)    | 7.0 (10)  | 852       | 252               | 122, 130  |

TABLE I. (Continued.)

| Energy [KeV] | Intensity | Placement |                  | Coincidences                       |
|--------------|-----------|-----------|------------------|------------------------------------|
|              |           | From      | To               |                                    |
| 602.7 (2)    | 16.0 (20) | 725       | 122              | 122                                |
| 614.2 (2)    | 12.1 (12) | 614       | 0                |                                    |
| 619.3 (4)    | 0.35 (5)  | (1277     | 658)             | (122), (536)                       |
| 639.9 (2)    | 8.3 (11)  | 762       | 122              | 122                                |
| 658.0 (4)    | 0.82 (10) | 658       | 0                |                                    |
| 660.6 (2)    | 0.76 (11) | 782       | 122              | 122                                |
| 671.7 (3)    | 0.67 (12) | 1433      | 762              | 122, (186), 640                    |
| 703.1 (3)    | 0.91 (18) | 1588      | 885              | 310, (576), 885                    |
| 706.7 (2)    | 2.33 (28) | 959       | 252              | 122, 130                           |
| 724.4 (2)    | 37.2 (44) | 725       | 0                |                                    |
| 730.4 (2)    | 3.67 (48) | 852       | 122              | 122                                |
| 761.6 (5)    | 2.10 (40) | 762       | 0                |                                    |
| 782.3 (2)    | 9.30 (80) | 782       | 0                |                                    |
| 805.7 (3)    | 0.57 (14) | 1588      | 782              | 782                                |
| 813.6 (4)    | 0.15 (8)  | 1066      | 252 <sup>m</sup> | (122)                              |
| 827.1 (2)    | 0.52 (8)  | 1079      | 252              | 122, 130                           |
| 830.8 (3)    | 0.45 (9)  | 1445      | 614              | 614                                |
| 836.8 (3)    | 0.25 (5)  | 959       | 122              | (122)                              |
| 857.7 (3)    | 0.41 (10) | 1433      | 576              | (454), (576)                       |
| 865.6 (3)    | 0.73 (10) | 1716      | 851              | 122, (130), 193, (275), (406), 536 |
| 883.6 (2)    | 2.42 (34) | 1006      | 122              | 122                                |
| 885.2 (3)    | 1.93 (48) | 885       | 0 <sup>n</sup>   |                                    |
| 929.5 (3)    | 3.1 (11)  | 1051      | 122              | 122                                |
| 929.8 (2)    | 3.39 (70) | 1588      | 658              | 122, 130, 406, 536                 |
| 938.5 (4)    | 0.39 (9)  | 1700      | 762              | (122), (640)                       |
| 942.9 (2)    | 2.86 (41) | 1065      | 122              | 122                                |
| 954.4 (3)    | 1.27 (22) | 1716      | 762              | 122, 640                           |
| 957.2 (2)    | 2.17 (31) | 1079      | 122              | 122                                |
| 967.6 (3)    | 1.47 (34) | 2401      | 1433             | 122, (1311)                        |
| 1003.8 (3)   | 0.55 (8)  | 1256      | 252              | 122, 130                           |
| 1005.5 (3)   | 4.20 (50) | 1006      | 0                |                                    |
| 1012.1 (1)   | 9.4 (10)  | 1588      | 576              | 122, 130, (324), 454, 576          |
| 1024.7 (3)   | 0.39 (7)  | 1147      | 122              | 122                                |
| 1041.7 (2)   | 0.94 (12) | 1700      | 658              | 122, 536                           |
| 1051.1 (3)   | 0.70 (30) | 1051      | 0                |                                    |
| 1064.7 (3)   | 8.00 (90) | 1065      | 0                |                                    |
| 1072.5 (3)   | 1.03 (20) | 1834      | 762              | 122, 640                           |
| 1074.6 (2)   | 0.31 (8)  | (1925     | 851)             | (193), (536)                       |
| 1079.0 (4)   | 1.70 (40) | 1079      | 0                |                                    |
| 1108.6 (2)   | 0.50 (10) | 1230      | 122              | 122                                |
| 1181.0 (4)   | 0.63 (11) | 1433      | 252              | 122, 130                           |
| 1220.2 (4)   | 0.37 (11) | 1834      | 614 <sup>a</sup> | (614)                              |
| 1311.1 (3)   | 0.80 (15) | 1433      | 122              | 122                                |
| 1317.2 (6)   | 0.36 (12) | 2079      | 762              | (122), (640)                       |
| 1397.3 (4)   | 0.47 (11) | 2449      | 1051             | (122), (930)                       |
| 1421.4 (4)   | 0.68 (11) | 2079      | 658              | 122, 536                           |
| 1548.5 (4)   | 0.81 (17) | (1670     | 122)             | (122)                              |
| 1548.9 (6)   | 0.42 (20) | (2401     | 852)             | (122), (194), (536)                |
| 1572.7 (4)   | 0.66 (23) | 2297      | 725              | (122), (725)                       |
| 1594.9 (4)   | 0.60 (40) | (1716     | 122)             | 122                                |
| 1596.6 (5)   | 0.65 (15) | 2449      | 852              | (194), (536)                       |
| 1597.6 (5)   | 0.19 (6)  | (2449     | 851)             | (193), (536)                       |
| 1629.2 (5)   | 0.54 (16) | 2297      | 668 <sup>a</sup> | (53), (92), (614)                  |
| 1639.0 (4)   | 0.75 (18) | 2401      | 762              | 122, 640                           |
| 1666.1 (4)   | 1.48 (31) | 2449      | 782              | 782                                |
| 1720.7 (7)   | 0.51 (16) | 2297      | 576              | (576)                              |

TABLE I. (Continued.)

| Energy [KeV] | Intensity | Placement |                  | Coincidences                   |
|--------------|-----------|-----------|------------------|--------------------------------|
|              |           | From      | To               |                                |
| 1724.4 (7)   | 0.58 (21) | 2449      | 725              | 122, (603), 725                |
| 1733.0 (4)   | 0.89 (28) | 2401      | 668 <sup>a</sup> | 53, (92), 122, 130, (415), 614 |
| 1742.7 (2)   | 3.49 (55) | 2401      | 658              | (82), 122, 130, 406, 536       |
| 1786.9 (4)   | 2.60 (68) | 2401      | 614 <sup>a</sup> | 614                            |
| 1790.6 (3)   | 2.16 (35) | 2449      | 658              | 122, 130, 406, 536             |
| 1833.7 (7)   | 0.17 (9)  | 2449      | 614 <sup>a</sup> | (614)                          |
| 1834.5 (5)   | 2.40 (7)  | 1834      | 0                |                                |
| 1870.0 (7)   | 0.29 (8)  | 2484      | 614 <sup>a</sup> | (614)                          |
| 1873.0 (6)   | 0.51 (15) | 2449      | 576              | 122, (454), (576)              |
| 1957.4 (4)   | 1.75 (35) | 2079      | 122              | 122                            |

<sup>a</sup>Reported in Ref. [10].

<sup>b</sup> $\gamma$  ray is not observed.  $I_{\gamma+e} = 2.4(8)$  units from 189-(53, 614) coincidences,  $M1$  [8].

<sup>c</sup> $\gamma$  ray is not observed.  $I_{\gamma+e} = 0.9(5)$  from 189-(406, 536) coincidences,  $E1$  [8].

<sup>d</sup>Modified placement agrees with Ref. [8].

<sup>e</sup> $E2$  [8].

<sup>f</sup> $M1$  assumed according to probable  $I^\pi$  for initial and final levels.

<sup>g</sup>Intensity is calculated from the coincidence counts with 1743 keV to avoid contamination by <sup>99</sup>Nb.

<sup>h</sup> $M1$  assumed.

<sup>i</sup> $M1$  [8].

<sup>j</sup>Another 215-keV transition [1] is not necessary owing to the new 275-keV transition.

<sup>k</sup>Was first reported in Ref. [8].

<sup>l</sup>Weak intermediate 639 keV is not observed.

<sup>m</sup>Only seen in coincidence with 122 keV. Could also be placed from level 2401 to 1588 keV.

<sup>n</sup>Adopted intensity deduced from coincidences is less than in singles.

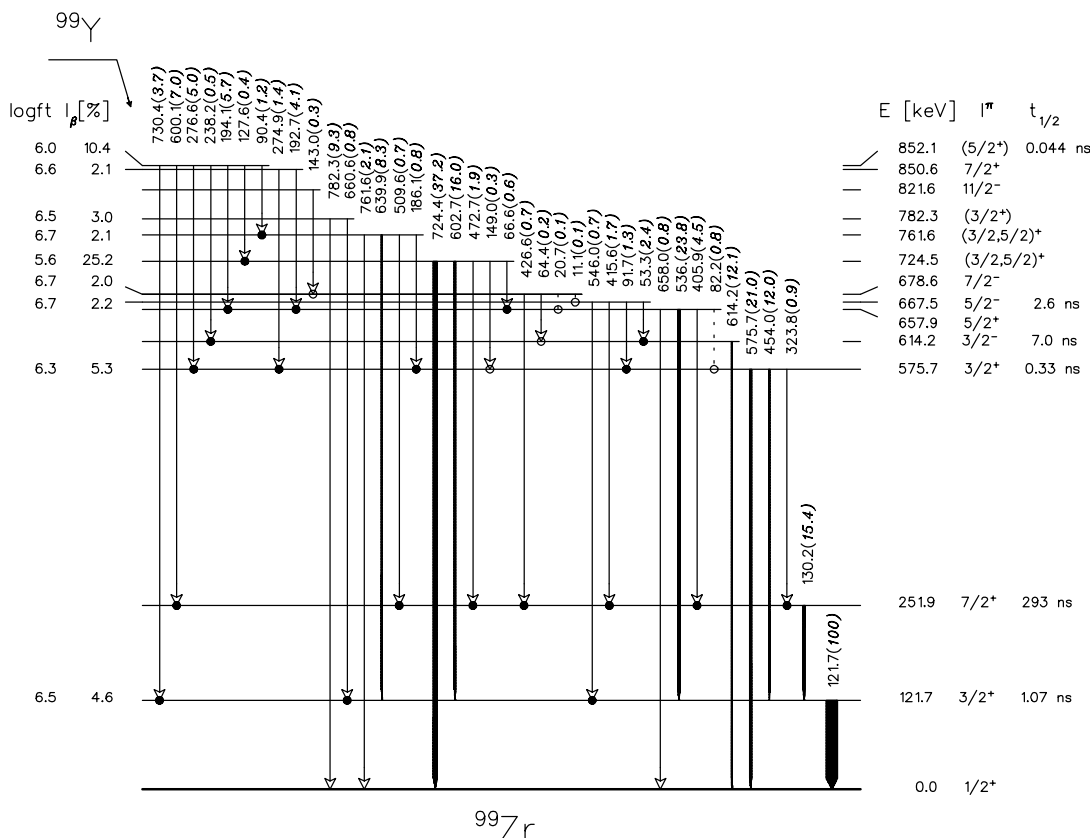


FIG. 3(a). Levels in <sup>99</sup>Zr populated in the decay of 5/2<sup>+</sup> <sup>99</sup>Y (lower part).

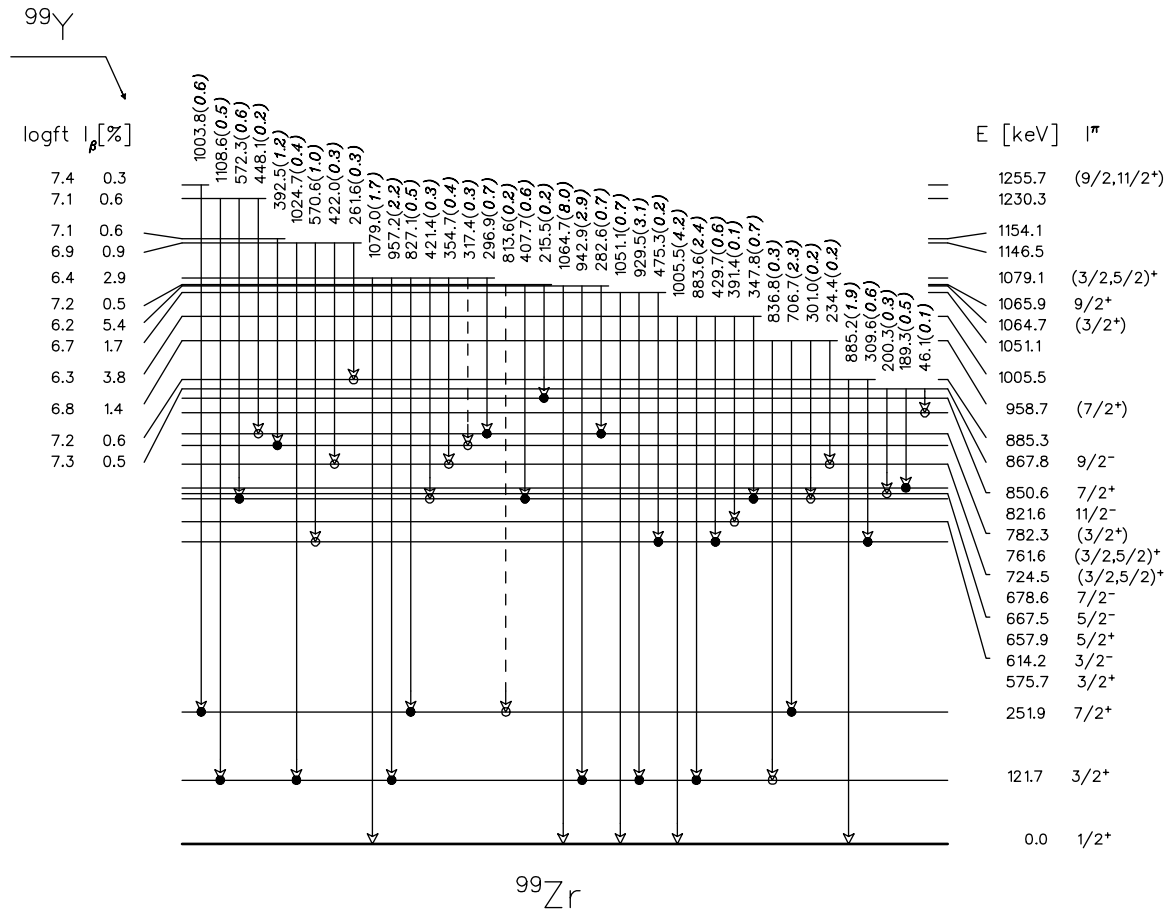


FIG. 3(b). Levels in <sup>99</sup>Zr populated in the decay of 5/2<sup>+</sup> <sup>99</sup>Y (middle part).

strongly coupled band [1]. The experimental  $\beta$ -feeding intensities,  $I_\beta(725) = 25.2\%$  and  $I_\beta(852) = 10.4\%$ , are in excellent agreement with  $I_\beta(852)/I_\beta(725) = 0.43$  resulting from the Alaga rule. The next  $I = K + 2$  band member is calculated to be weakly directly populated (1.8%) and be near 1030 keV if the moment of inertia of the postulated band is constant. However, and despite the improved quality of the data, no experimental level being clearly suitable has been found.

Comparison with prompt fission data shows that the highest spins directly populated are 9/2<sup>+</sup> (1066 keV) and 9/2<sup>-</sup> (867 keV). The log(ft) values indicate that a weak fraction of their  $\gamma$ -ray feeding (especially of the 1066 keV level) still has been overlooked. The 11/2<sup>-</sup> level at 822 keV is populated by the 46-keV transition from the 9/2<sup>-</sup> level, in agreement with the placement by Urban *et al.* [8], and has no sizable direct  $\beta$  feeding. The 9/2<sup>+</sup> level at 1039 keV recently reported as the [404]9/2 neutron orbital [9] is not populated strongly enough to be observed. We note the 1256-keV level with a single transition to the 7/2<sub>1</sub><sup>+</sup> state at 252 keV and little  $\beta$  feeding. These properties could have allowed its identification as the 11/2<sup>+</sup> level at 1257 keV belonging to the 9/2 band known from Ref. [9]. However, neither the 11/2<sup>+</sup>-to-9/2<sup>+</sup> transition nor those depopulating the 9/2<sup>+</sup> state have been observed. Thus, the 1256-keV transition is probably not the one observed in prompt fission.

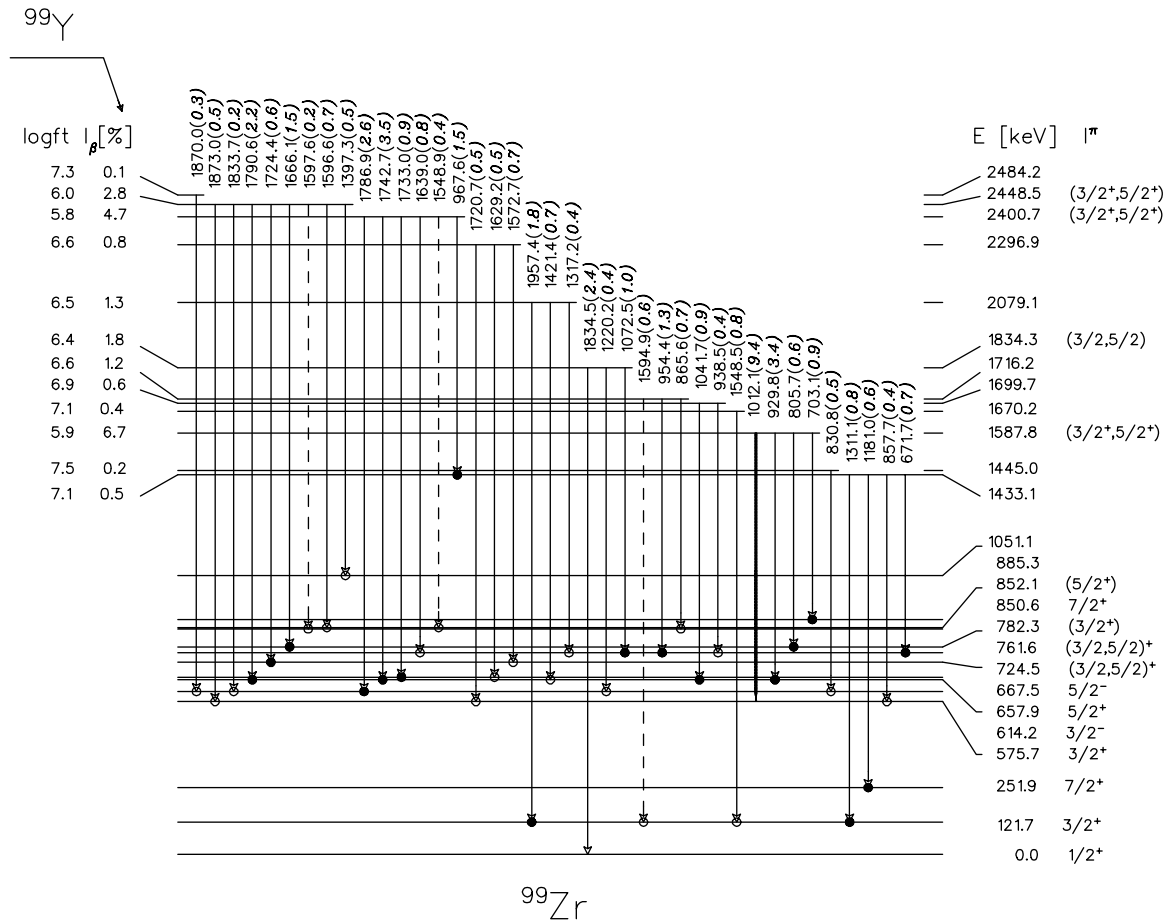
#### IV. DISCUSSION

The low-lying levels of <sup>99</sup>Zr are spherical with  $\nu s_{1/2}$  associated with the ground state and  $\nu g_{7/2}$  with the second excited state at 252 keV. Particular attention has been devoted to the 3/2<sup>+</sup> first excited state at 122 keV of more complex character [4,16]. The  $K = 3/2$  odd-parity band [1,8,10] is very irregular at low spin. This is a consequence of its  $h_{11/2}$  parentage. It is interesting to note that it has been possible to reproduce the pattern in a IBFM calculation despite the modest flexibility of the model in the SU(3) limit [17].

The small number of definite spin and parity assignments for the <sup>99</sup>Zr levels observed in  $\beta$  decay does not favor an unambiguous discussion supported by model calculations. The search for similarities within neighboring  $N = 59$  isotones could be the way to get some insight into these levels. The level systematics of the even-even neighbors of <sup>99</sup>Zr shows the influence of the  $d_{5/2}$  shell closure near  $N = 56$  and the development of large g.s. deformations at  $N = 60$  for Zr and Sr neutron-rich isotopes but not for molybdenum. We therefore discuss the relationships of <sup>99</sup>Zr levels with their possible counterparts in <sup>97</sup>Sr.

##### A. Experimental comparison with <sup>97</sup>Sr

Most of the levels observed in  $\beta$  decay of <sup>99</sup>Y are logically 3/2<sup>+</sup> or 5/2<sup>+</sup> states fed by allowed  $\beta$  transitions from the

FIG. 3(c). Levels in  $^{99}\text{Zr}$  populated in the decay of  $5/2^+$   $^{99}\text{Y}$  (upper part).

$5/2^+$  g.s. or  $\gamma$  cascades. Such states can be generated by coupling the spherical  $1/2^+$  ground state, the next  $3/2_1^+$  and  $7/2_1^+$  to core excitations ( $E(0_2^+) = 854$  keV,  $E(2_1^+) = 1223$  keV [18]). In addition, an extra pair of  $(3/2^+, 5/2^+)$  states is expected as the  $I = K$  and  $K + 1$  levels of the  $[422]3/2$  Nilsson orbital by analogy with  $^{97}\text{Sr}$ . In that nucleus the  $7/2^+(822) \rightarrow 5/2^+(687) \rightarrow 3/2^+(585)$  cascade has been interpreted as a strongly coupled band, based on the presence of an enhanced  $E2$  component in the  $5/2 \rightarrow 3/2$  transition of 102 keV [2, 19]. As already mentioned, the 725- and 852-keV levels in  $^{99}\text{Zr}$  have been assumed in Ref. [1] to be the corresponding  $3/2^+$  and  $5/2^+$  levels of that band. Figure 4 shows possible correspondences of levels in  $^{97}\text{Sr}$  and  $^{99}\text{Zr}$ . The links are based on the similarities of branching ratios of the depopulating transitions, together with the recent report of some of these levels as being members of bands of similar characteristics in  $^{97}\text{Sr}$  and  $^{99}\text{Zr}$  [8]. We note that the 725- and 762-keV levels in  $^{99}\text{Zr}$  have not been observed in prompt fission. The 576-keV level, assigned  $I^\pi = 3/2^+$  by Urban *et al.* [8], turns out to be a better candidate for the level similar to the 585-keV level in  $^{97}\text{Sr}$ . The finite half-life of 0.33(2) ns measured for the 576-keV level [15] results in a rate of 0.6 Weisskopf units for the g.s. transition if pure  $E2$ . This upper limit indicates a slow rate that is hardly consistent with the spherical  $2^+ \otimes s_{1/2}$  configuration, even if the collectivity of the  $2_1^+$  states in this region is remarkably weak [20]. The

658-keV level could be tentatively the next band member with  $I^\pi = 5/2^+$ . However, whether the expected  $K = 3/2^+$  band head is the 725- or the 576-keV level, the supposedly  $K + 1 \rightarrow K$  transition is very weak. The failure to observe a  $5/2^+ \rightarrow 3/2^+$  transition with a large branching ratio casts doubts about the existence of a strongly coupled  $3/2^+$  band in  $^{99}\text{Zr}$ . Urban *et al.* indeed present the levels at 576 and 658 keV as the  $K = 3/2$  and  $5/2$  heads of decoupled bands [8].

As a matter of fact, the branching ratios of the 725-keV level also indicate the 601-keV level in  $^{97}\text{Sr}$  as the possible corresponding level. The latter has been interpreted as a spherical core + particle level with  $I^\pi = 5/2^+$  [19]. This opens the way for another interpretation of the 725-keV level (i.e., the  $2^+ \otimes s_{1/2}$  configuration). In the case of nondeformation, the arguments for  $I^\pi(725) = 3/2^+$  do not apply anymore and one can consider  $I^\pi = 5/2^+$  as well. The other level of this configuration is possibly the  $(3/2, 5/2)$  762-keV level, corresponding to the 522-keV  $(3/2^+, 5/2^+)$  level in  $^{97}\text{Sr}$ . Both have transitions to the  $1/2_1^+$ ,  $3/2_1^+$ , and  $7/2_1^+$  states, with the transition to the  $3/2_1^+$  state being the strongest. It is logical to assume the core + particle states to be higher in energy in  $^{99}\text{Zr}$  [ $E(2_1^+, ^{98}\text{Zr}) = 1223$  keV] than in  $^{97}\text{Sr}$  [ $E(2_1^+, ^{96}\text{Sr}) = 815$  keV]. The levels mentioned above (i.e., the pairs 601–725 and 522–762) follow this trend. We therefore examine the possibility for these levels to be

TABLE II. Levels fed in the decay of  $^{99}\text{Y}$ .  $T_{1/2} = 1.5$  s,  $Q_{\beta} = 7.60$  MeV are used to calculate  $\log(ft)$  values. The ground-state  $\beta$  branching is assumed to be negligible.

| Energy [KeV] | $\beta$ feeding % | $\log(ft)$ | $t_{1/2}$ [ns] | $I^{\pi}$            | Configuration |
|--------------|-------------------|------------|----------------|----------------------|---------------|
| 0.0          | 0.00              |            |                | $1/2^{+}$            | $s_{1/2}^a$   |
| 121.7(1)     | 4.58(218)         | 6.5        | 1.07(3)        | $3/2^{+}$            |               |
| 251.9(2)     | 0.24(127)         | 7.8        | 293(10)        | $7/2^{+}$            | $8_{7/2}^b$   |
| 575.7(1)     | 5.34(179)         | 6.3        | 0.33(2)        | $3/2^{+}$            |               |
| 614.2(2)     | 0.75(72)          | 7.2        | 7.0(9)         | $3/2^{-}$            | $[541]3/2^c$  |
| 657.9(1)     | 2.07(150)         | 6.7        |                | $5/2^{+}$            |               |
| 667.5(1)     | 2.21(54)          | 6.7        | 2.6(14)        | $5/2^{-}$            |               |
| 678.6(2)     | 1.99(45)          | 6.7        | 8.9(12)        | $7/2^{-}$            |               |
| 724.5(1)     | 25.2(20)          | 5.6        |                | $(3/2, 5/2)^{+}$     |               |
| 761.6(2)     | 2.11(59)          | 6.7        |                | $(3/2, 5/2)^{+}$     |               |
| 782.3(2)     | 3.01(43)          | 6.5        |                | $(3/2^{+})$          |               |
| 821.6(4)     | 0.06(5)           | 8.2        |                | $11/2^{-}$           |               |
| 850.6(2)     | 2.13(27)          | 6.6        |                | $7/2^{+}$            |               |
| 852.1(1)     | 10.4(8)           | 6.0        | 0.04 (1)       | $(5/2^{+})$          |               |
| 867.8(2)     | 0.51(6)           | 7.3        |                | $9/2^{-}$            |               |
| 885.3(2)     | 0.60(25)          | 7.2        |                |                      |               |
| 958.7(2)     | 1.37(15)          | 6.8        |                | $(7/2^{+})$          |               |
| 1005.5(2)    | 3.81(33)          | 6.3        |                |                      |               |
| 1051.1(2)    | 1.68(53)          | 6.7        |                |                      |               |
| 1064.7(2)    | 5.40(51)          | 6.2        |                | $(3/2^{+})$          |               |
| 1065.9(2)    | 0.47(7)           | 7.2        |                | $9/2^{+}$            |               |
| 1079.1(1)    | 2.91(28)          | 6.4        |                | $(3/2, 5/2)^{+}$     |               |
| 1146.5(2)    | 0.92(10)          | 6.9        |                |                      |               |
| 1154.1(4)    | 0.56(8)           | 7.1        |                |                      |               |
| 1230.3(2)    | 0.62(8)           | 7.1        |                |                      |               |
| 1255.7(4)    | 0.26(4)           | 7.4        |                | $(9/2, 11/2^{+})$    |               |
| 1433.1(2)    | 0.49(20)          | 7.1        |                |                      |               |
| 1445.0(4)    | 0.21(4)           | 7.5        |                |                      |               |
| 1587.8(1)    | 6.67(64)          | 5.9        |                | $(3/2^{+}, 5/2^{+})$ |               |
| 1699.7(3)    | 0.62(8)           | 6.9        |                |                      |               |
| 1716.2(2)    | 1.22(22)          | 6.6        |                |                      |               |
| 1834.3(3)    | 1.78(35)          | 6.4        |                | $(3/2, 5/2)$         |               |
| 2079.1(3)    | 1.31(19)          | 6.5        |                |                      |               |
| 2296.9(3)    | 0.80(15)          | 6.6        |                |                      |               |
| 2400.7(2)    | 4.69(51)          | 5.8        |                | $(3/2^{+}, 5/2^{+})$ |               |
| 2448.5(2)    | 2.82(29)          | 6.0        |                | $(3/2^{+}, 5/2^{+})$ |               |
| 2484.2(7)    | 0.14(4)           | 7.3        |                |                      |               |

<sup>a</sup>The structure of this state is complex [4].

<sup>b</sup>Member of even-parity band [8].

<sup>c</sup>Member of the odd-parity band [8].

described in the interacting boson fermion framework as spherical states based on the  $2^{+} \otimes s_{1/2}$  configuration.

### B. IBFM calculation of $^{97}\text{Sr}$ and $^{99}\text{Zr}$

The interacting-boson-fermion model has been previously applied in the description of spherical states in  $^{97}\text{Sr}$  [2] and  $^{99}\text{Zr}$  [4]. In the analysis of Refs. [2] and [4] very limited information on the level spectra and electromagnetic properties of  $^{97}\text{Sr}$  and  $^{99}\text{Zr}$  was used to determine the fermion-boson interaction strengths, effective charges, and gyromagnetic factors. For the lowest three positive parity states,  $1/2_{1}^{+}$ ,  $3/2_{1}^{+}$ , and  $7/2_{1}^{+}$ , the theoretical description was very good. At an

excitation energy of approximately 600 keV the IBFM calculations in both nuclei predicted a pair of  $3/2_{2}^{+}$  and  $5/2_{1}^{+}$  spherical states predominantly based on the  $2^{+} \otimes s_{1/2}$  configuration. In the present work we attempt to assign these states to the levels at 522 and 601 keV (in  $^{97}\text{Sr}$ ) and 725 and 762 keV (in  $^{99}\text{Zr}$ ), using the corresponding wave functions from calculations in Refs. [2] and [4]. For both nuclei we use the same effective charges and  $g$  factors, namely those from the former calculation of the low-lying levels of  $^{99}\text{Zr}$  [4]. In calculating branching ratios the experimental energies of the transitions have been applied, in accordance with the usual practice in the theoretical analysis of electromagnetic decays. The electromagnetic transitions in both nuclei are dominated by  $l$ -forbidden  $M1$  and low-collective  $E2$  terms and therefore



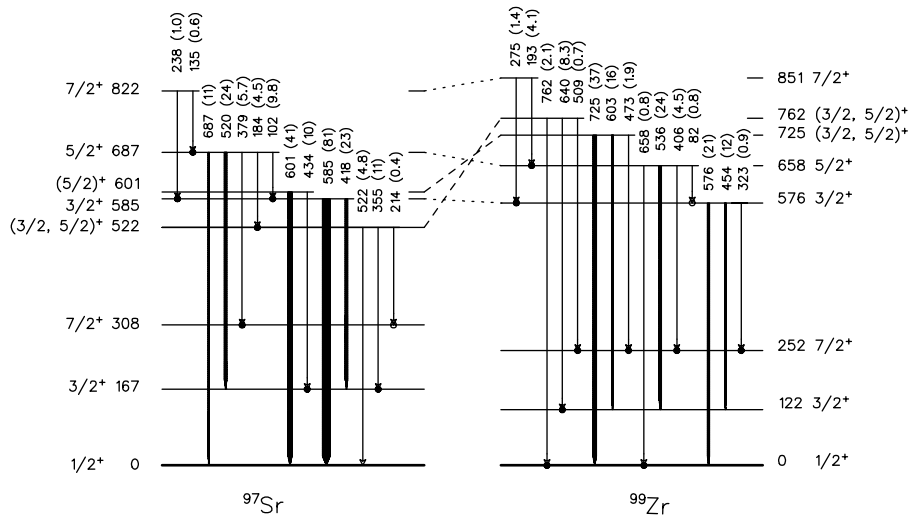


FIG. 4. Even-parity levels in the  $N = 59$  isotones  $^{97}\text{Sr}$  and  $^{99}\text{Zr}$  discussed in the text. Not all transitions are shown. Intensities are those observed in  $\beta$  decay. The dotted lines indicate the states forming decoupled  $3/2^+$  and  $5/2^+$  bands according to Ref. [8], but also interpreted as a strongly coupled  $K = 3/2^+$  band in  $^{97}\text{Sr}$  [2,19]. The dashed lines connect possible spherical  $2^+ \otimes s_{1/2}$  levels, see Ref. [19] for  $^{97}\text{Sr}$ .

are characterized by small transition probabilities that are sensitive to the details of the model parametrization and to contributions from outside the model space. The contribution that is neglected assuming a subshell closure at  $Z = 38$  can be attributed to proton components in the internal structure of the boson. This contribution is more undervalued in  $^{97}\text{Sr}$  than in  $^{99}\text{Zr}$ , resulting in a description of the states above the low-lying  $1/2_1^+$ ,  $3/2_1^+$ ,  $7/2_1^+$  levels better in  $^{99}\text{Zr}$  than in  $^{97}\text{Sr}$ . Therefore, for states above 0.5 MeV a qualitative (specially in  $^{97}\text{Sr}$ ), rather than a quantitative, agreement for branching ratios can be expected. Tables III (for  $^{97}\text{Sr}$ ) and IV (for  $^{99}\text{Zr}$ ) show the experimental and calculated branching ratios for the  $3/2_2^+$  and  $5/2_1^+$  states belonging to the  $2^+ \otimes s_{1/2}$  configuration. The predominant decay of the  $3/2_2^+$  state into the  $3/2_1^+$  state, makes it a good candidate for the 522-keV level in  $^{97}\text{Sr}$ . The assignment of the 601 keV level in  $^{97}\text{Sr}$  to the  $2^+ \otimes s_{1/2}$  based  $5/2^+$  state, in accordance with  $5/2^+$  from Ref. [19], is fair if the limitations of the calculation are considered. The rate of the  $E2$  transition to the ground state is underestimated by a factor of about 8. The competing transition to the  $3/2_1^+$  state is calculated to be the strongest one and the level half-life of 56 ps is a factor 5 above the experimental upper limit. The results for IBFM branching ratios in  $^{99}\text{Zr}$  are in good agreement with the experimental values. They favor an assignment of  $5/2^+$  for the 725-keV level and  $3/2^+$  for the 762-keV level.

TABLE III. Branching ratios for decays of possible spherical  $2^+ \otimes s_{1/2}$  levels (labeled as  $3/2_s^+$  and  $5/2_s^+$ ) of  $^{97}\text{Sr}$ .

| Level [keV] | Assignment $I^\pi$ | Decay to  | Branching ratio |      |
|-------------|--------------------|-----------|-----------------|------|
|             |                    |           | Experiment      | IBFM |
| 522         | $3/2_s^+$          | $1/2_1^+$ | 44              | 7    |
|             |                    | $3/2_1^+$ | 100             | 100  |
|             |                    | $7/2_1^+$ | 4               | 0.01 |
| 601         | $5/2_s^+$          | $1/2_1^+$ | 100             | 100  |
|             |                    | $3/2_1^+$ | 24              | 188  |
|             |                    | $7/2_1^+$ | —               | 6    |
|             |                    | $3/2_s^+$ | —               | 21   |

The IBFM predictions for the ordering of  $5/2^+$  and  $3/2^+$   $2^+ \otimes s_{1/2}$  levels in both nuclei [2,4] show an inversion, the  $5/2^+$  level being above the  $3/2_2^+$  level in  $^{97}\text{Sr}$  and conversely in  $^{99}\text{Zr}$ . This scheme is in accordance with the analysis of transitions. We can conclude that the predicted properties of the  $3/2^+$  and  $5/2^+$  states based on the  $2^+ \otimes s_{1/2}$  configuration in  $^{97}\text{Sr}$  and  $^{99}\text{Zr}$  [2,4] are in a qualitative agreement with their experimental counterparts proposed in this work.

Finally, it might be worth examining if the  $3/2^+$  and  $5/2^+$  states observed in prompt fission as the lowest levels of bands [8] could correspond to the spherical  $2^+ \otimes s_{1/2}$  states. The band structure implies a correspondance of the 576-keV ( $3/2^+$ ) and 658-keV ( $5/2^+$ ) levels with the 585- and 687-keV levels in  $^{97}\text{Sr}$ . A half-life,  $t_{1/2}(687) = 0.36(2)$  ns [2,19], has been measured for the  $5/2^+$  state in  $^{97}\text{Sr}$ . The deduced enhancement of the  $E2$  component in the  $5/2^+ \rightarrow 3/2^+$  transition of 102 keV is not consistent with a transition between spherical  $2^+ \otimes s_{1/2}$  levels. The IBFM branching ratios from these levels, if spherical, are similar to those shown in Tables III and IV, a fact that reflects the similar transition energies and is little conclusive. The calculated half-life of the  $5/2^+$  level in  $^{97}\text{Sr}$ , 30 ps, is a factor 12 times shorter than the experimental value. Thus, the calculated probabilities of the transitions into the spherical  $1/2_1^+$ ,  $3/2_1^+$ , and  $7/2_1^+$  states, which altogether represent about 70% of the decay intensity, are near an order of magnitude larger than the

TABLE IV. Branching ratios for decays of possible spherical  $2^+ \otimes s_{1/2}$  levels (labeled as  $3/2_s^+$  and  $5/2_s^+$ ) of  $^{99}\text{Zr}$ .

| Level [keV] | Assignment $I^\pi$ | Decay to  | Branching ratio |      |
|-------------|--------------------|-----------|-----------------|------|
|             |                    |           | Experiment      | IBFM |
| 725         | $5/2_s^+$          | $1/2_1^+$ | 100             | 100  |
|             |                    | $3/2_1^+$ | 43              | 41   |
|             |                    | $7/2_1^+$ | 5               | 7    |
| 762         | $3/2_s^+$          | $1/2_1^+$ | 25              | 19   |
|             |                    | $3/2_1^+$ | 100             | 100  |
|             |                    | $7/2_1^+$ | 8               | 0.4  |
|             |                    | $5/2_s^+$ | —               | 0.2  |

experimental ones. These discrepancies indicate that the 585- and 687-keV level hardly can be associated with the spherical  $2^+ \otimes s_{1/2}$  levels and, consequently, neither their counterparts in  $^{99}\text{Zr}$ . We note that the calculated half-life of 25 ps for the  $3/2^+$  spherical level in  $^{99}\text{Zr}$ , assumed at 576 keV, is also an order of magnitude too small with respect to the experimental value of 0.33(2) ns. It is therefore improbable that the 576- and 658-keV levels are an alternative to the 725- and 762-keV levels for being the spherical states. On this basis, and within the limitations of the model, the most likely assignments have been made for the spherical  $3/2^+$  and  $5/2^+$  levels.

## V. CONCLUSION

The new investigation of the decay scheme of  $^{99}\text{Y}$  to  $^{99}\text{Zr}$  has been performed with less contamination of  $\beta$ -decay precursors and better spectrum quality than the last performed study. It allows a more reliable level scheme to be constructed. The differences with the former results, however, only involve removal of the weakest transitions or addition of new ones at a level of a percentage of relative intensity units. These marginal revisions anyway improve the agreement with the recently published prompt-fission data.

Whereas shape coexistence in  $^{99}\text{Zr}$  has been recently well established with the observation of the [404]9/2 Nilsson orbital in prompt fission, a definite signature for the earlier postulated

deformed band built on the [422]3/2 Nilsson orbital still is lacking. In contrast to former interpretation, despite its strong feeding in the decay of the strongly deformed  $^{99}\text{Y}$  mother nucleus, suggesting an allowed transition toward a deformed  $3/2^+$  state, the 725-keV level does not appear as the head of a band. On the basis of analogies of low-spin levels in  $^{97}\text{Sr}$  and  $^{99}\text{Zr}$  and predictions of the interacting boson fermion model the 725-keV level could be a spherical  $2^+ \otimes s_{1/2}$  level. There is no definite argument to assign a spin to the 725-keV level nor to its probable partner within the  $2^+ \otimes s_{1/2}$  configuration assumed to be the level at 762 keV. In any case, the description of shape coexistence in the transition region of ground-state deformation at  $N=59$  still requires extensive experimental effort going beyond standard spectroscopic measurements. In particular, dedicated lifetime and angular correlations measurements could help to unravel the complexity of the level structure of  $^{99}\text{Zr}$ .

## ACKNOWLEDGMENTS

Part of the data presented here have been obtained at the IGISOL on-line separator at Jyväskylä, Finland. The authors thank Drs. P. Dendooven, J. Huikari, H. Penttilä, and K. Peräjärvi for performing the mass separation and Dr. P. Jones for assistance in constructing the  $\gamma$ - $\gamma$  matrices.

- 
- [1] G. Lhersonneau, B. Pfeiffer, K.-L. Kratz, T. Enqvist, P. P. Jauho, A. Jokinen, J. Kantele, M. Leino, J. M. Parmonen, H. Penttilä, and J. Äystö, *Phys. Rev. C* **49**, 1379 (1994).
- [2] G. Lhersonneau, B. Pfeiffer, K.-L. Kratz, H. Ohm, K. Sistemich, S. Brant, and V. Paar, *Z. Phys. A* **337**, 149 (1990).
- [3] S. Brant, V. Paar, G. Lhersonneau, O. W. B. Schult, H. Seyfarth, and K. Sistemich, *Z. Phys. A* **334**, 517 (1989).
- [4] S. Brant, V. Paar, and A. Wolf, *Phys. Rev. C* **58**, 1349 (1998).
- [5] G. Lhersonneau, S. Brant, and V. Paar, *Phys. Rev. C* **62**, 044304 (2000).
- [6] P. Campbell, H. L. Thayer, J. Billowes, P. Dendooven, K. T. Flanagan, D. H. Forest, J. A. R. Griffith, J. Huikari, A. Jokinen, R. Moore, A. Nieminen, G. Tungate, S. Zemlyanoi, and J. Äystö, *Phys. Rev. Lett.* **89**, 082501 (2002).
- [7] J. H. Hamilton, A. V. Ramayya, S. J. Zhu, G. M. Ter-Akopian, Yu. Oganessian, J. D. Cole, J. O. Rasmussen, and M. A. Stoyer, *Prog. Part. Nucl. Phys.* **35**, 635 (1995).
- [8] W. Urban, J. L. Durell, A. G. Smith, W. R. Phillips, M. A. Jones, B. J. Varley, T. Rząca-Urban, I. Ahmad, L. R. Morss, M. Bentele, and N. Schulz, *Nucl. Phys.* **A689**, 605 (2001).
- [9] W. Urban, J. A. Pinston, T. Rząca-Urban, A. Zlomaieci, G. Simpson, J. L. Durell, W. R. Phillips, A. G. Smith, B. J. Varley, I. Ahmad, L. R. Morss, and N. Schulz, *Eur. Phys. J. A* **16**, 11 (2003).
- [10] G. Lhersonneau, P. Dendooven, A. Honkanen, M. Huhta, P. M. Jones, R. Julin, S. Juutinen, M. Oinonen, H. Penttilä, J. R. Persson, K. Peräjärvi, A. Savelius, J. C. Wang, and J. Äystö, *Phys. Rev. C* **56**, 2445 (1997).
- [11] G. Lhersonneau, J. Suhonen, P. Dendooven, A. Honkanen, M. Huhta, P. Jones, R. Julin, S. Juutinen, M. Oinonen, H. Penttilä, J. R. Persson, K. Peräjärvi, A. Savelius, J. C. Wang, J. Äystö, S. Brant, V. Paar, and D. Vretenar, *Phys. Rev. C* **57**, 2974 (1998).
- [12] R. A. Meyer, E. Monnard, J. A. Pinston, F. Schussler, I. Ragnarsson, B. Pfeiffer, H. Lawin, G. Lhersonneau, T. Seo, and K. Sistemich, *Nucl. Phys.* **A439**, 510 (1985).
- [13] G. Lhersonneau, P. Dendooven, G. Cachel, J. Huikari, P. Jardin, A. Jokinen, V. Kolhinen, C. Lau, L. Lebreton, A. C. Mueller, A. Nieminen, S. Nummela, H. Penttilä, K. Peräjärvi, Z. Radivojević, V. Rubchenya, M.-G. Saint-Laurent, W. H. Trzaska, D. Vakhtin, J. Vervier, A. C. C. Villari, J. C. Wang, and J. Äystö, *Eur. Phys. J. A* **9**, 385 (2000).
- [14] F. K. Wohn, J. C. Hill, C. B. Howard, K. Sistemich, R. F. Petry, R. L. Gill, H. Mach, and A. Piotrowski, *Phys. Rev. C* **33**, 677 (1986).
- [15] H. Ohm *et al.*, quoted in L. K. Peker, revise Nucl. Data Sheets **73**, 1 (1994).
- [16] A. Wolf, R. L. Gill, Z. Berant, and D. S. Brenner, *Phys. Rev. C* **51**, 2381 (1995).
- [17] S. Brant, G. Lhersonneau, and K. Sistemich, *Phys. Rev. C* **69**, 034327 (2004).
- [18] B. Singh and Z. Hu, *Nucl. Data Sheets* **98**, 335 (2003).
- [19] M. Büscher, R. F. Casten, R. L. Gill, R. Schuhmann, J. A. Winger, H. Mach, M. Moszynski, and K. Sistemich, *Phys. Rev. C* **41**, 1115 (1990).
- [20] H. Mach, F. K. Wohn, G. Molnár, K. Sistemich, J. C. Hill, M. Moszynski, R. L. Gill, W. Krips, and D. S. Brenner, *Nucl. Phys.* **A523**, 197 (1991).